JOURNAL OF GEOPHYSICAL RESEARCH, VOL. 101, NO. D21, PAGES 26,347–26,361, NOVEMBER 27, 1996

Model for multiscale disaggregation of spatial rainfall based on coupling meteorological and scaling descriptions

S. Perica[1] and E. Foufoula-Georgiou

St. Anthony Falls Laboratory, Department of Civil Engineering, University of Minnesota, Minneapolis

Abstract. The precipitation output of a mesoscale atmospheric numerical model is usually interpreted as the average rainfall intensity over the grid cell of the model (typically 30×30 km to 60×60 km). However, rainfall exhibits considerable heterogeneity over subgrid scales (i.e., scales smaller than the grid cell), so it is necessary for hydrologic applications to recreate or simulate the small-scale rainfall variability given its large-scale average. Rainfall disaggregation is usually done statistically. In this paper, a new subgrid scale rainfall disaggregation model is developed. It has the ability to statistically reproduce the rainfall variability at scales unresolved by mesoscale models while being conditioned on large-scale rainfall averages and physical properties of the prestorm environment. The model is based on two extensively tested hypotheses for midlatitude mesoscale convective systems [*Perica and Foufoula-Georgiou,* 1996]: (1) standardized rainfall fluctuations (defined via a wavelet transform) exhibit simple scaling over the mesoscale, and (2) statistical scaling parameters of rainfall fluctuations relate to the convective available potential energy (CAPE), a measure of the convective instability of the prestorm environment. Preliminary evaluation of the model showed that the model is capable of reconstructing the small-scale statistical variability of rainfall as well as the fraction of area covered with rain at all analyzed subgrid scales. The performance evaluation was based on comparison of summary statistics and spatial pattern measures of simulated fields with those of known fields observed during the Oklahoma-Kansas Preliminary Regional Experiment for Storm-Central (PRE-STORM).

1. Introduction

The last decade has witnessed substantial improvements in our ability to physically model rainfall at the mesoscale (horizontal scale of the order of a few kilometers to several hundred kilometers) and global scale (horizontal scale larger than a couple of hundred kilometers). Despite considerable progress, however, rainfall still remains one of the most difficult variables to predict in meteorological models. This limits the accuracy with which other hydrologic variables, such as runoff, can be modeled or predicted. Moreover, the results of physically based meteorological models (mesoscale weather prediction models or global circulation models (GCMs)) are available only at large grid scales, much coarser than those needed for hydrologic applications at the basin and subbasin scale (typically less than a few kilometers in horizontal scale). In addition, the spatial heterogeneity of rainfall within a GCM or mesoscale model grid cell considerably affects the state of the atmosphere and mass balances over that cell, making it thus desirable to incorporate the subgrid-scale variability of rainfall in the dynamics of climate models themselves. Rainfall disaggregation at the unresolved (subgrid) scales is commonly treated statistically. Some rainfall subgrid-scale parameterization schemes for GCM models are available (see, for example, *Thomas and Henderson-Sellers* [1991] for a review), but fewer exist for mesoscale models.

The proposed approach for rainfall subgrid-scale parameterization is conceptually different from current approaches used in GCM models. It is based upon two main hypotheses: (1) that standardized rainfall fluctuations, defined via an orthogonal Haar wavelet transform of the original rainfall field, exhibit simple scaling

[1]Now University Corporation for Atmospheric Research (UCAR) visiting scientist at NOAA/NWS/Hydrologic Research Laboratory, Silver Spring, Maryland.

Paper number 96JD01870.
0148-0227/96/96JD-01870$09.00

over the mesoscale, and (2) that the scaling parameters of standardized rainfall fluctuations relate to thermodynamic descriptors of the prestorm environment. These two hypotheses were extensively tested in a previous paper by the authors [*Perica and Foufoula-Georgiou,* 1996] using data from the Oklahoma-Kansas Preliminary Regional Experiment for Storm-Central (PRE-STORM) field program that took place in May and June 1985 (see *Cunning* [1986] for more details on that program).

The structure of the present paper is as follows: In section 2 we briefly summarize the basic hypotheses on which we built our model and present the relations between statistical parameterizations and thermodynamic parameters of the prestorm environment obtained for mesoscale convective systems (the reader is referred to the original publication of *Perica and Foufoula-Georgiou* [1996], for more details). In section 3 we give the model description and a step-by-step procedure for model implementation. In section 4, criteria for judging model performance are established. Based on the selected criteria, the model is tested on the 0300 UTC, June 27, 1985 PRE-STORM data set. In section 5 we perform a sensitivity analysis on the same data set. Finally, in section 6 a brief summary of the developed model and its performance is given.

2. Summary of Scaling and Predictive Relationships

Let $X(t_1, t_2)$ represent the two-dimensional spatially continuous rainfall field and $\overline{X}_m(i,j)$ its discrete local average value at relative scale m and location (i,j). The correspondence of relative scale m to physical scale in kilometers is given in Table 1. The smallest scale of 4×4 km (m=0) corresponds to the resolution of the radar rainfall observations and the largest scale of 64×64 km (m=4) reflects our desire to have enough averaging cells within the radar picture for a meaningful statistical analysis at that scale. It also corresponds to the resolution at which a current numerical mesoscale model can comfortably provide rainfall averages (which we seek to disaggregate). Note from Table 1 that the increase in physical scale is dyadic for convenience in implementing discrete multiscale algorithms.

The discrete field $\overline{X}_m(i,j)$ is "filtered" through four two-dimensional orthogonal filters (Φ, Ψ_1, Ψ_2, and Ψ_3), called the scaling and directional wavelet filters, respectively (see *Kumar and Foufoula-Georgiou* [1993a, b] and *Perica and Foufoula-Georgiou* [1996]). This operation produces an average field $\overline{X}_{m+1}(n,k)$ at the next higher scale (m+1) and three directional "fluctuation" fields at that same higher scale $\{X'_{m+1,i}(n,k)\}_{i=1,2,3}$. The indices (i,j) define spatial position at scale m, while the indices (n,k) define spatial position at the next higher scale (m+1), as illustrated in Figure 1. The three "fluctuation" fields capture high frequencies in the vertical, horizontal, and diagonal directions in the frequency domain and thus can be seen as capturing "edges" in the vertical, horizontal, and diagonal directions (i=1,2,3, respectively) in the physical domain.

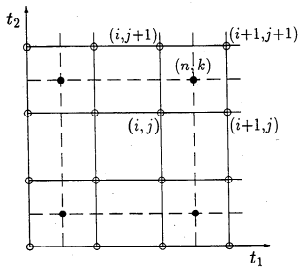

Figure 1. Schematic showing discretization on a two-dimensional grid at relative scales m and (m+1). Open circles define spatial positions at scale m and solid circles define spatial positions at next higher scale (m+1).

Let us fix ideas by considering the first scale of decomposition from relative scale m=0 (here 4×4 km, the radar data resolution) to the next higher (dyadic) scale (here 8×8 km). Introducing indices (i,j) to define spatial position at scale m=0 and (n,k) to define spatial position at scale m=1 (see Figure 1), the average process $X_0(i,j) \equiv \overline{X}_0(i,j)$ at the initial scale of 4×4 km is decomposed to $\overline{X}_1(n,k)$ the average field at the next higher scale of 8×8 km, and $\{X'_{1,i}(n,k)\}_{i=1,2,3}$ the three directional fluctuation components at the same higher scale. If a Haar wavelet is chosen for the decomposition [see *Kumar and Foufoula-Georgiou* [1993a] and *Perica and Foufoula-Georgiou,* 1996], the average process at scale m=1 is computed as

$$\overline{X}_1(n,k) = \frac{1}{4}[\overline{X}_0(i,j) + \overline{X}_0(i,j{+}1) + \overline{X}_0(i{+}1,j) + \overline{X}_0(i{+}1,j{+}1)], \quad (1)$$

and the three fluctuation components as

$$X'_{1,1}(n,k) = \frac{1}{4}\{[\overline{X}_0(i,j) + \overline{X}_0(i,j{+}1)] - [\overline{X}_0(i{+}1,j) + \overline{X}_0(i{+}1,j{+}1)]\} \quad (2)$$

$$X'_{1,2}(n,k) = \frac{1}{4}\{[\overline{X}_0(i,j) + \overline{X}_0(i{+}1,j)] - [\overline{X}_0(i,j{+}1) + \overline{X}_0(i{+}1,j{+}1)]\} \quad (3)$$

$$X'_{1,3}(n,k) = \frac{1}{4}\{[\overline{X}_0(i,j) - \overline{X}_0(i{+}1,j)] - [\overline{X}_0(i,j{+}1) - \overline{X}_0(i{+}1,j{+}1)]\}. \quad (4)$$

As can be seen from the above equations, rainfall fluctuations admit an easy interpretation: they can be seen as discrete representations of $\partial\overline{X}_0/\partial t_1$, $\partial\overline{X}_0/\partial t_2$ and $\partial^2\overline{X}_0/\partial t_1\partial t_2$ (where position indices have been dropped for convenience). Therefore they correspond to a scheme widely used for defining gradients of two-dimensional processes. At the same time, $\overline{X}_1$ is exactly

equal to the two-dimensional average of the rainfall process from the previous scale. This procedure is repeated on the process $\overline{X}_1$ to obtain the average process $\overline{X}_2$ and three directional rainfall fluctuations $\{X'_{2,i}\}_{i=1,2,3}$ at the relative scale m=2, and so on.

On the basis of the analysis of several storms from the PRE-STORM data set it was found [*Perica and Foufoula-Georgiou,* 1996] that rainfall fluctuations, when standardized by the corresponding-scale rainfall averages, that is,

$$\xi_{m,i} = \begin{cases} X'_{m,i}/\overline{X}_m & \text{if } \overline{X}_m > 0 \\ 0 & \text{if } \overline{X}_m = 0, \end{cases} \qquad (5)$$

consistently exhibit Gaussianity and statistical simple-scaling behavior within the range of scales considered (4 to 64 km). This results in a statistical representation of the standardized rainfall fluctuations which, in general, consists of six parameters: standard deviations $\sigma_{1,i}$ at scale 1 (here at scale 8×8 km) and scale invariant exponents H_i, for each of the three directional components (i=1,2,3). Parameters $\sigma_{1,i}$ relate to the variability of the standardized rainfall fluctuations at relative scale m=1 and parameters H_i dictate how the variability of standardized rainfall fluctuations changes over scales, through equation

$$\sigma_{m,i} = 2^{(m-1)H_i}\,\sigma_{1,i} \qquad m \geq 1 \qquad (6)$$

resulting from the simple scaling condition (see *Perica and Foufoula-Georgiou* [1996] for more details and for interpretation of these parameters).

To explore whether the proposed scaling parameterization for standardized rainfall fluctuations depends on the storm type, *Perica and Foufoula-Georgiou* [1996] classified the PRE-STORM data sets as either stratiform or convective, based on the dominant precipitation mechanisms. Among convective events, a further distinction was made between linear systems (squall lines) and all other systems that do not exhibit a linear structure, termed chaotic [*Blanchard,* 1990]. First, we found that scaling of standardized rainfall fluctuations was present over the same range of scales (8 to 64 km), independent of storm type. Second, we found that for stratiform systems the estimated H_i values were in the range of 0.14–0.18, and the estimated $\sigma_{1,i}$ values were in the range of 0.44–0.53. For convective systems, the H_i values were higher (approximately 0.20–0.45) and the $\sigma_{1,i}$ values were lower (in the range of 0.15 to 0.50). Among convective systems, we could not clearly distinguish differences in the parameters of chaotic and linear systems. The scaling parameters were found to be more dependent on the severity of the storm rather than on the specific storm type; severe storms had higher H_i and smaller $\sigma_{1,i}$ estimates. In most cases, directional differences among parameters were insignificant and parameterization was approximated by only two parameters: H and σ_1. However, for some linear convective systems the directional differences were too significant to be ignored. For more details the reader is referred to the original publication of *Perica and Foufoula-Georgiou* [1996].

The hypothesis set forward by *Perica and Foufoula-Georgiou* [1996] was that the parameterization of standardized rainfall fluctuations, being dependent on the storm intensity, might be related to parameters describing physical characteristics of the storm environment. The validity of this hypothesis was tested using 17 PRE-STORM data sets for which simultaneous radar scans and radiosonde soundings were available. Linear regression analysis was used to quantify relations between the scaling parameters H and σ_1 and a number of thermodynamic and kinematic parameters describing the prestorm environment. The best correlations were obtained with a single thermodynamic parameter, the convective available potential energy (CAPE):

$$H = 0.0516 + 0.9646(\text{CAPE} \times 10^{-4}) \qquad (7)$$

$$\sigma_1 = 0.5390 - 0.8526(\text{CAPE} \times 10^{-4}) \qquad (8)$$

having correlation coefficients R=0.82 and R=-0.73, respectively. In the above equations, CAPE is in square meters per square second, and H and σ_1 are dimensionless. The average potential temperature and the mixing ratio in the lowest 50 mbar were used to define the characteristics of the surface parcel used in computing the CAPE values. The scattergram of CAPE and H with the indicated regression line is shown in Figure 2a, and of CAPE and σ_1 in Figure 2b. These relationships are seen as applicable to midlatitude mesoscale convective systems and for values of CAPE between 1000 and 3000 m^2/s^2. They are explored in this research for the purpose of developing subgrid-scale rainfall parameterization models, that is, models that can resolve the rainfall variability at scales smaller than those resolved by a mesoscale numerical weather prediction model (typically 30 to 60 km).

3. Model Development

3.1. Theoretical Basis

The theoretical basis of the proposed subgrid-scale disaggregation model lies on the findings summarized in section 2 (see also *Perica and Foufoula-Georgiou* [1996], for more details), namely, the Gaussianity and simple scaling of standardized rainfall fluctuations (equation (6)) and the predictive relationships between scaling parameters H and σ_1 and CAPE (equations (7) and (8)). The Haar wavelet transform is a perfect reconstruction filter; that is, given the rainfall average process $\overline{X}_m$ at scale m and the corresponding fluctuation processes $\{X'_{m,i}\}_{i=1,2,3}$ at the same scale, the rainfall process at the next lower scale (m-1) can be reconstructed exactly via the inverse Haar wavelet transform. So, given the rainfall average process at a large (coarse) scale (say at 32×32 km) and the rainfall fluctuations at that and all finer scales (32×32, 16×16, and 8×8 km), one would

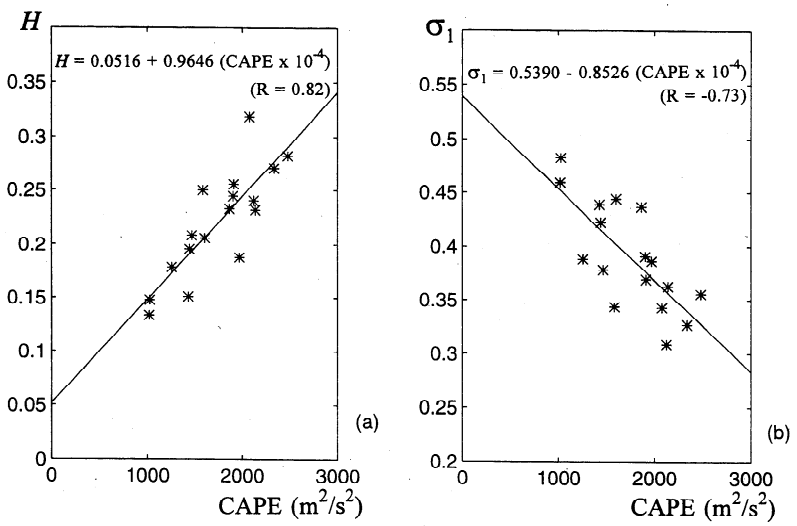

Figure 2. Scattergrams with indicated regression lines and correlation coefficients (a) for the convective available potential energy (CAPE) and H and (b) for CAPE and σ_1.

be able to reconstruct via the inverse wavelet transform the rainfall process at the finest scale (here 4×4 km) or any intermediate scale. Of course, if the rainfall fluctuation fields are not given exactly but rather statistically (here parameterized via statistical simple scaling of their standardized values) then a statistical reconstruction of rainfall at any desired fine scale can be obtained. This is exactly the idea behind our proposed model.

The model requires as input a large-scale rainfall average process, say rainfall averages on 32×32 or 64×64 km grids, and also CAPE values from the prestorm environment. Both of these inputs are envisioned to be provided by the output of a mesoscale numerical weather prediction model. Then, based on an inverse wavelet procedure and on the statistical scaling and predictive relationships established for mesoscale convective systems (equations (6), (7), and (8)), rainfall intensities at any desired scale (say 16×16 km, 8×8 km, or 4×4 km) can be computed recursively (through inverse wavelet transform), from large to small scales. Section 3.2 gives a step-by-step procedure of the model implementation.

3.2. Implementation Procedure

The following procedure explains how one can implement the proposed model for rainfall disaggregation at subgrid scales. The flow chart of the procedure is given in Figure 3.

Step 1: Initialization. The model is initialized with large-scale average rainfall intensities (e.g., averages over 32×32 or 64×64 km; relative scale index m=M) and soundings from which representative CAPE values (i.e., values which would reasonably represent the average level of convective instability in the prestorm environment) can be estimated. For computational efficiency, initial-scale rainfall averages should be given for

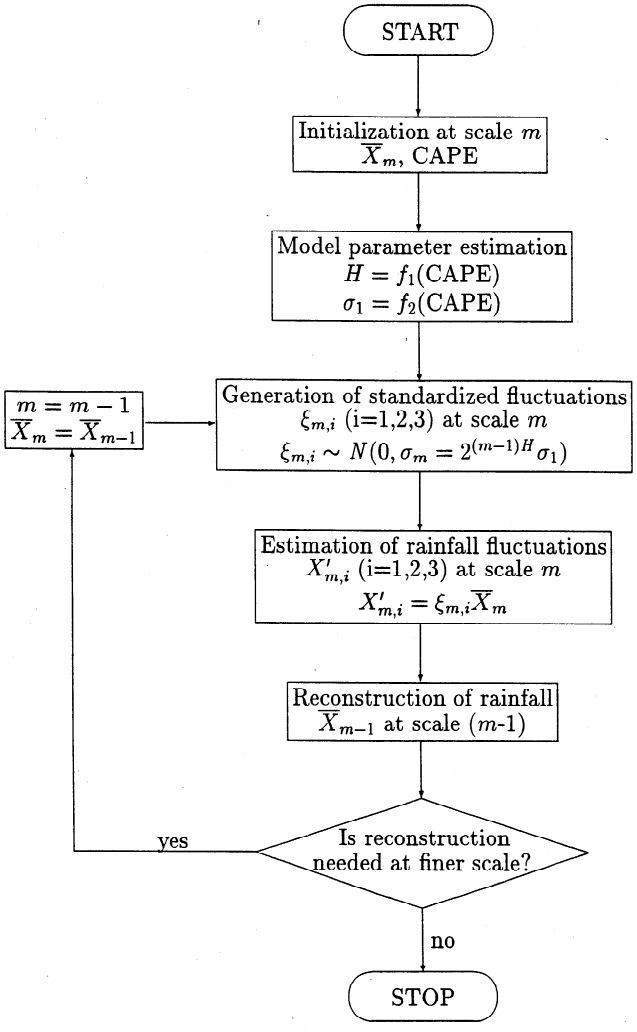

Figure 3. Flow chart for the disaggregation procedure.

N×N boxes where N=2^j ($j \geq 0$). If necessary, empty boxes can be filled with zeros to satisfy this condition.

Step 2: Parameter estimation. The model parameters H and σ_1 are estimated from the previously established predictive equations with CAPE (here equations (7) and (8) for midlatitude convective systems).

Step 3: Generation of standardized fluctuations. Three N×N spatially independent truncated (between -1 and 1) Gaussian fields with zero mean and standard deviation $\sigma_m = 2^{(m-1)H}\sigma_1$ are used for the generation of the standardized fluctuations $\{\xi_{m,i}\}_{i=1,2,3}$. Truncation is used to accommodate the fact that fluctuations obtained from a nonnegative field, such as rainfall, via the Haar wavelet transform are always smaller or, at most, equal to the corresponding average field. Since by definition standardized fluctuations are ratios between fluctuations and average rainfall, they have to be distributed between [-1,1]. This restriction might present a problem only in cases of $\sigma_m > 0.5$ - 0.6, because in these cases a mass greater than $\approx 5 - 7\%$ of the Gaussian distribution $N(0, \sigma_m)$ will fall outside [-1,1]. For our midlatitude mesoscale systems the model-predicted σ_m values exceeded the value of 0.6 only slightly for scales of 64×64 km and small values of CAPE (see Figure 11 – dashed lines). Based on this alone, it is suggested that the proposed disaggregation model is initiated at scales smaller than 64×64 km and, preferably, at scales 32×32 km.

Step 4: Estimation of rainfall fluctuations. Rainfall fluctuations $\{X'_{m,i}\}_{i=1,2,3}$ are obtained as products of the generated standardized fluctuations $\xi_{m,i}$ and corresponding rainfall averages $\overline{X}_m$ (i.e., $X'_{m,i} = \xi_{m,i}\overline{X}_m$). Notice that this operation results in zero fluctuations for all boxes that have estimated zero average rainfall.

Step 5: Reconstruction of rainfall. To reconstruct a rainfall field at the next finer scale (m-1), an inverse wavelet transform is used to "add" generated fluctuations $X'_{m,i}$ to the corresponding averages $\overline{X}_m$. The algorithm for reconstructing rainfall is based on the two-dimensional inverse wavelet algorithm developed by *Mallat* [1989]. It is illustrated by a block diagram shown in Figure 4 and described in the following six steps: (1) A column of zeros is added between each two columns of $\overline{X}_m$ and $\{X'_{m,i}\}_{i=1,2,3}$. (2) Each row is convolved with a one-dimensional filter ϕ or ψ, as indicated in Figure 4. The filters used for the inverse Haar wavelet transform are given in Figure 5. (3)The resulting filtered fields are summed as indicated in Figure 4: the filtered field $\overline{X}_m$ with $X'_{m,2}$ and the filtered field $X'_{m,1}$ with $X'_{m,3}$. (4) A row of zeros is added between each of the two resulting fields. (5) Each column of both resulting fields is convolved with either filter ϕ or ψ, as indicated in the block diagram. (6) Both filtered fields are summed to reconstruct the rainfall field at scale (m-1). The size of the reconstructed field at scale (m-1) is 2^2 times larger the size of the rainfall field at relative scale m. If the reconstruction of rainfall is needed at a finer scale, the current scale (m-1) becomes a scale with relative index m, and steps 3 to 5 are repeated. This procedure may be repeated as many times as necessary. A schematical presentation of the rainfall reconstruction procedure over m scales is given in Figure 6.

Using this algorithm, it is possible to reconstruct a rainfall field which includes negative rainfall intensities. Theoretically, rainfall intensities generated with a two-dimensional inverse Haar wavelet transform might have

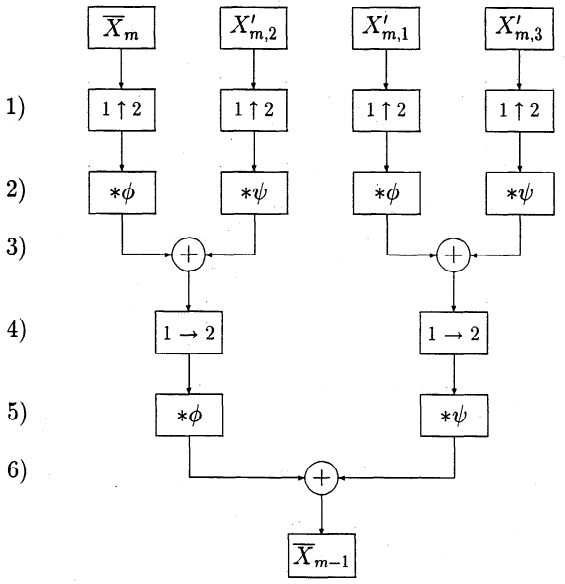

Figure 4. Two-dimensional inverse wavelet transform for reconstruction of $\overline{X}_{m-1}$ from $\overline{X}_m$ and $\{X'_{m,i}\}_{i=1,2,3}$.

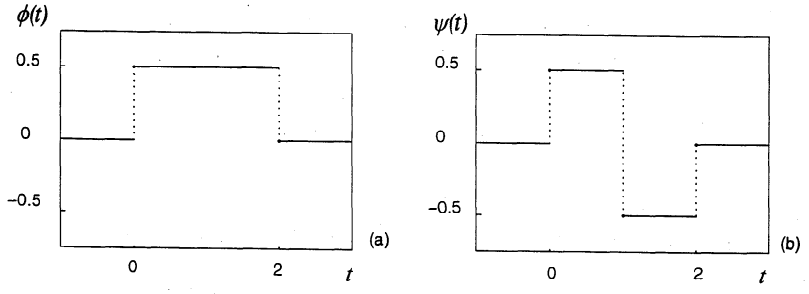

Figure 5. Filters (a) ϕ and (b) ψ used for the inverse Haar wavelet transform.

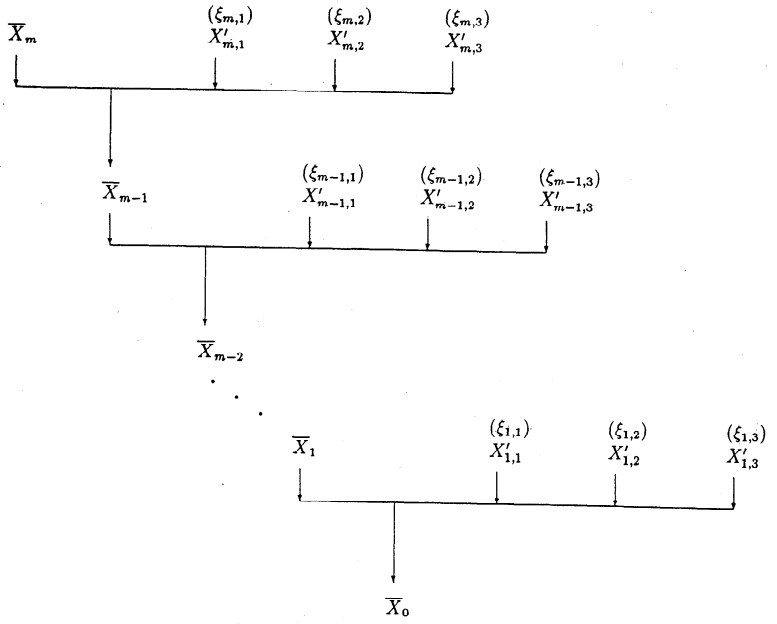

Figure 6. Schematic showing rainfall reconstruction procedure.

negative magnitudes of up to twice the order of magnitude of the corresponding average rainfall intensity from the previous scale. However, the probability of generating a significant number of significantly lower than zero rainfall intensities is very small (it corresponds to the probability of simultaneous generation of three Gaussian numbers from the tails of their distribution). Thus, in our simulations the very small number of generated negative rainfall intensities was set to zero after careful checking of their magnitudes and position.

3.3. Intermittency Preservation Via Thresholding

The importance of fractional wetting in determining the response of a hydrologic system was demonstrated by *Johnson et al.* [1990]. Generally, the fraction of area covered with rain is a function of the scale at which rainfall is represented; as scale decreases that fraction also decreases, and vice versa (see also *Kumar and Foufoula-Georgiou* [1994]). Commonly, it is assumed (e.g., in GCMs) that the fraction of area covered with rain changes exponentially over scales. It is represented through an empirically defined parameter ranging between zero and one. As mentioned earlier, the inverse wavelet transform permits exact reconstruction of the rainfall process and its intermittency at any scale if all three fluctuation components were known exactly at the scale at which we started reconstruction and at all intermediate scales up to one scale larger than the scale of interest. However, rainfall fluctuations are not known exactly but rather are generated in the way described in section 3.2. Thus there is no a priori condition in the wavelet methodology that could guarantee intermittency reconstruction. However, we found that when simple thresholding on the reconstructed average field is performed, the model performs remarkably well in reconstructing rainy and nonrainy areas. This threshold value can be seen as an additional parameter of the proposed disaggregation model which can be estimated empirically. For example, for our data sets we estimated this parameter by investigating model performance with several threshold values τ= 0.1, 0.25, 0.5, 0.75, and 1.0 mm/h applied at every scale. Figure 7 shows the fraction of area covered by rain as a function of scale for all these thresholds and for the 0300 UTC, June 27, 1985, PRE-STORM data set. Based on similar analysis of several other PRE-STORM data sets, an optimal threshold value of τ=0.25 mm/h was empirically estimated and is recommended for subgrid scale disaggregation of midlatitude convective systems.

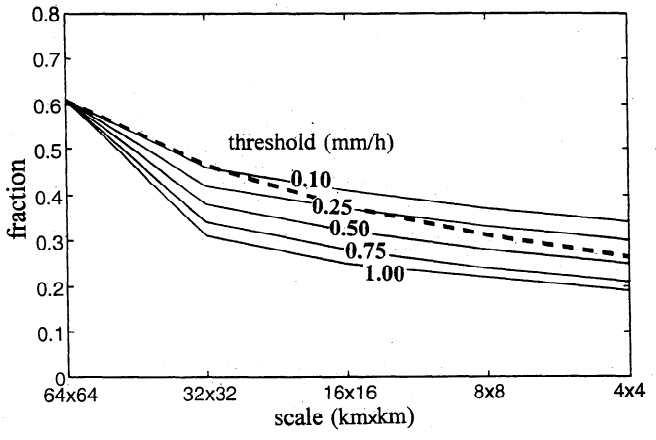

Figure 7. The 0300 UTC, June 27, 1985, data set. Reconstruction of fractional coverage of rain for different threshold values used in the reconstruction process. The dashed line is computed from the original data set.

In our simulations, the mass of rainfall lost in thresholding, although generally insignificant, was redistributed to other nonzero rainfall intensities generated from the same average rainfall from the previous scale to preserve the average rainfall inside each box. This redistribution was done proportionally to the generated rainfall amounts in each box.

4. Model Performance Evaluation

4.1. Criteria for Evaluation

To quantify the agreement between the observed and the modeled (disaggregated) fields, two general classes of criteria were used: (1) statistical measures and (2) pattern comparison. Since this is a statistical model and statistical variation of the output results is expected, we ran the disaggregation model 100 times (i.e., produced 100 disaggregated fields from the same initial conditions and parameters) and compared the results of both a single simulation and the ensemble of simulations to the "true" fields at all dyadic scales from 32×32 km up to 4×4 km (relative scales m=3,2,1,0) (see Table 1).

1. Statistical agreement was based on statistical properties of (1) the rainfall field $\overline{X}_m$ at relative scale m with zero intensities included and (2) the strictly nonzero rainfall field $\overline{R}_m$. It is reminded that $\overline{X}_m$ refers to the average rainfall intensities over the grid boxes corresponding to scale m; same applies for $\overline{R}_m$. Statistical properties of these average values over the domain of the radar umbrella is what we use in the sequel for model evaluation. Specifically, the following statistical properties were considered: mean, $\overline{\overline{X}}_m = E[\overline{X}_m]$; conditional mean, $\overline{\overline{R}}_m = E[\overline{X}_m | \overline{X}_m > 0] = E[\overline{R}_m]$; variance, $\sigma^2_{\overline{X},m} \equiv \sigma^2[\overline{X}_m] = E[\overline{X}^2_m] - E^2[\overline{X}_m]$; conditional variance, $\sigma^2_{\overline{R},m} \equiv \sigma^2[\overline{R}_m] = E[\overline{R}^2_m] - E^2[\overline{R}_m]$; conditional nonexceedance probability, $F(r) = Pr(\overline{R}_m < r)$; and conditional spatial correlation. Conditional spatial correlation represents standardized covariance calculated with the assumption that the rainfall field is second-order stationary (that is, covariance is independent of the location, but it does depend on the distance and orientation). Notice that statistical comparison, based on conditional moments only, depends to a certain extent on the degree of the approximation of the fraction of the area covered with rain. For example, a valuable feature of the Haar wavelet transform is an exact preservation of the unconditional average rainfall intensities at all scales; not only is the average rainfall preserved over the whole domain of interest but it is also preserved locally inside each box from one scale to the next smaller scale. However, if the size of the wetted area in the model is significantly underestimated or overestimated, the average value of the modeled nonzero rainfall field could significantly differ from the original (true) average value. In addition to the aforementioned statistics, scattergrams of modeled versus observed values (sorted in ascending order) were displayed relative to the 1:1 line of perfect correspondence. Sorting was done to compare the magnitudes of observed and modeled intensities regardless of their positions.

2. The pattern comparison was based on: a visual comparison of observed and modeled images, a spatial "figure of merit" measure, and a comparison of the size of the wetted area for observed and simulated fields. A "look and see" approach, i.e., a visual comparison of observed and modeled images, is a good first step, and a very efficient one in determining if the modeled rainfall fields look realistic. The "figure of merit" index was suggested, for example, by *Klug et al.* [1992] for the analysis of spatial patterns. This dimensionless index is defined as the area of the intersection of the observed and predicted areas, divided by the union of these two areas. It has a theoretical range of 0.0 (for no agreement) to 1.0 (for perfect agreement).

Table 1. Range of Scales Used in This Study, Their Relative Indices, and the Size of the Available Data Sets at Each Scale

Physical Scale (km×km)	Relative Scale m	Size of the Data Set
4×4	0	128×128
8×8	1	64×64
16×16	2	32×32
32×32	3	16×16
64×64	4	8×8

4.2. Results of Model Performance Evaluation: A Case Study

The 0300 UTC, June 27 data set from a long-lived (> 16 hours) mesoscale convective system (MCS) that produced heavy rainfall was selected for model performance evaluation. This MCS was one of the most extensively studied events in our previous analysis that explored relations between scaling parameterization and quantities describing the prestorm environment (see *Perica and Foufoula-Georgiou* [1996] for more details). There were three reasons for selecting this storm: (1) because of the slow movement of this MCS the precipitation was within the range of Kansas and Oklahoma radars for almost its entire life cycle, (2) the areal coverage of the event was large enough to be used in scaling analysis for more than 10 hours, and (3) stability indices calculated from sounding stations located within the western and central portions of the PRE-STORM network did not exhibit significant differences, so we could estimate representative (average) values of the indices with more confidence. Finally, at 0300 UTC the storm, now in its mature-to-dissipating stage, had a well-formed hier-

Table 2. Statistical Moment Estimates for Observed (O) and Modeled (M_1 and M_{100} For One Simulation and 100 Simulations, Respectively) Rainfall Fields at All Analyzed Scales

Statistical Moment Estimates		Scale (km×km)				
		64×64	32×32	16×16	8×8	4×4
$\overline{\overline{X}}$, mm/h	(O)	1.84	1.84	1.84	1.84	1.84
	(M_1)		1.84	1.84	1.84	1.84
	(M_{100})		1.84	1.84	1.84	1.84
$\sigma_{\overline{X}}$, mm/h	(O)	3.11	3.83	4.93	5.70	6.59
	(M_1)		3.94	4.77	5.64	6.51
	(M_{100})		3.81 (0.21)	4.62 (0.26)	5.48 (0.29)	6.39 (0.34)
$\overline{\overline{R}}$, mm/h	(O)	3.02	3.96	4.93	5.93	6.97
	(M_1)		4.40	5.13	5.74	6.34
	(M_{100})		4.36 (0.13)	5.01 (0.17)	5.63 (0.18)	6.21 (0.20)
$\sigma_{\overline{R}}$, mm/h	(O)	3.51	4.83	7.07	8.96	11.30
	(M_1)		5.42	6.67	8.92	11.20
	(M_{100})		4.85 (0.39)	6.51 (0.52)	8.41 (0.63)	10.50 (0.78)

The 0300 UTC, June 27, 1985, data set. For the 100 simulations the average moment values and their standard deviations (number in parentheses) are given. Note that the unconditional mean $\overline{\overline{X}}$ is exactly preserved at all scales by model construction.

archical pattern that we wanted to test how well the model could mimic.

The model input parameters were rainfall average intensities at the 64×64 km scale (obtained by aggregating the 4×4 km Oklahoma radar rainfall intensities) and a CAPE value of 1584 m^2/s^2 measured at 0300 UTC at the Henryetta (HET) station located approximately 10 km ahead of the storm convection region. The developed model was used to produce (simulate) disaggregated rainfall fields at all intermediate scales, i.e., 32×32, 16×16, 8×8, and 4×4 km. Model performance evaluation, by comparing single-simulation runs

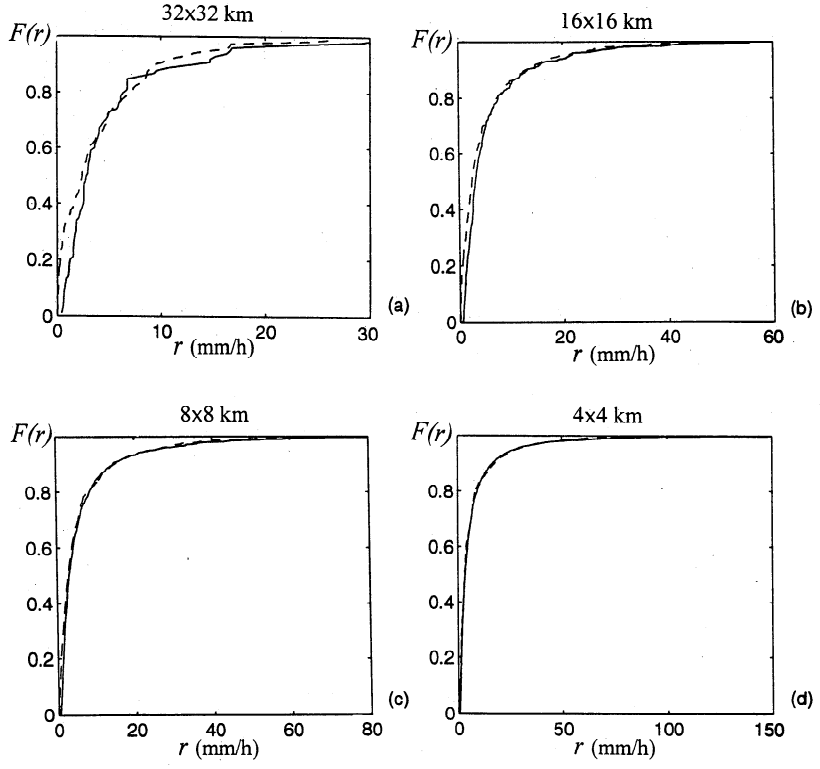

Figure 8. The 0300 UTC, June 27, 1985, data set. Conditional nonexceedance probability curves (see text for definition) of observed data set (solid line) and simulated data set (dashed line), given at all scales of reconstruction.

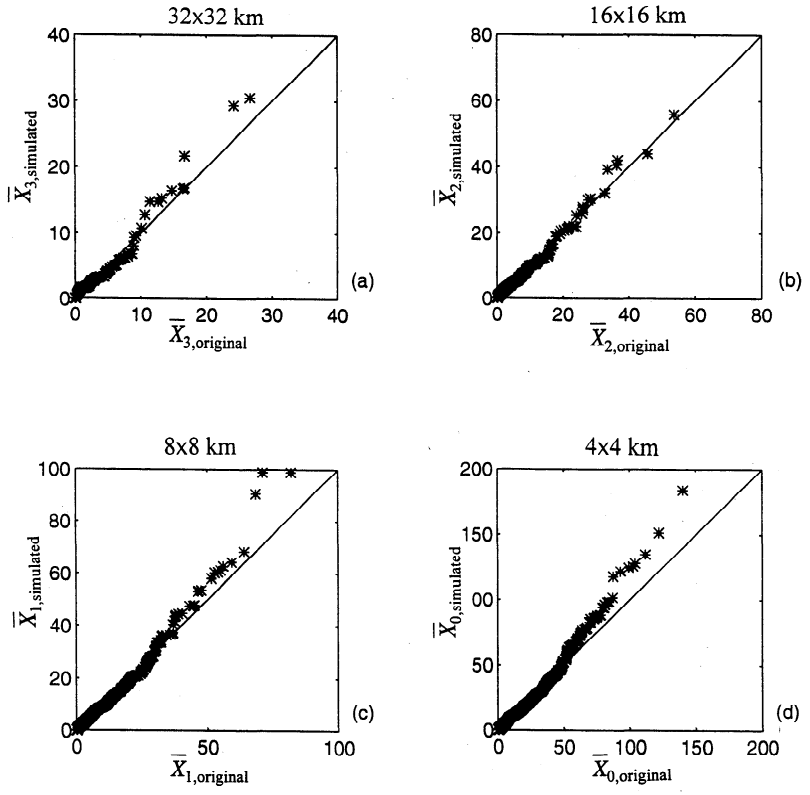

Figure 9. The 0300 UTC, June 27, 1985, data set. Scattergrams of simulated versus original rainfall intensities sorted in ascending order, relative to the "perfect correspondence" line. Intensities (in millimeters per hour) are compared for scales 32×32 up to 4×4 km, respectively.

and an ensemble of simulations to the "true" fields, was done at all analyzed scales. Table 2 lists the statistical moment estimates for the observed and modeled fields at all four scales. For the modeled field we list two types of moment estimates: from one specific simulation and the average values and standard deviations of moment estimates from 100 simulations. As can be seen from the table, the modeled statistical measures are comparable with those observed throughout all scales. Moreover, there is virtually no difference in the moment estimates obtained from one run and those obtained from the average of estimates of 100 runs (also evidenced from the small standard deviation of these estimates).

The conditional nonexceedance probabilities of the observed and predicted fields are shown in Figures 8a-8d. In each figure, the true rain rate distribution function is given by the solid line and the simulated rain rate distribution function by the dashed line. As shown in the figure, the model does a very good job of reproducing the observed conditional rainfall probabilities; there is very little difference in the estimated and observed curves.

A similar type of model-accuracy testing was performed by comparing scattergrams of measured intensities with those of one particular simulation. Intensities were sorted in ascending order, and as shown in Figure 9, the paired intensities produced an almost perfect line with unit slope passing through the origin. There was only a slight deviation from that line at high rain rates, which is the result of the overestimation of the highest rainfall intensity at the 32×32 km scale that was transmitted down to finer scales.

Figure 10 shows the spatial correlation structure of simulated and observed rainfall fields. Despite the generally good agreement it seems that there exists a constant tendency for the autocorrelation of the simulated fields to decrease more rapidly than that of the observed fields. The reason is that the simulated small-scale rainfall field does not usually achieve the "connectivity" (a measure of the relative positions of zero and nonzero rainfall intensities, i.e., holes) of the actual rainfall field. Further improvements of the algorithm (implemented after submission of this paper) suggest that the preservation of the autocorrelation function in the simulated fields can be significantly improved by repositioning the simulated rainfall intensities obtained inside each box from a previous scale using a simple connectivity rule applied to their neighbors.

The spatial rainfall patterns also compare relatively well, as shown in Plate 1. Plate 1a represents the average rainfall field at 64×64 km with which we initialized our simulation. As can be seen from Plate 1, there is good agreement in the rain patterns of the simulated and original field at all scales. The "figure of merit" measure over all four scales is given in Table 3 for one simulation and for 100 simulations (average and standard deviation). As can be seen from the table, the agreement between simulated and measured

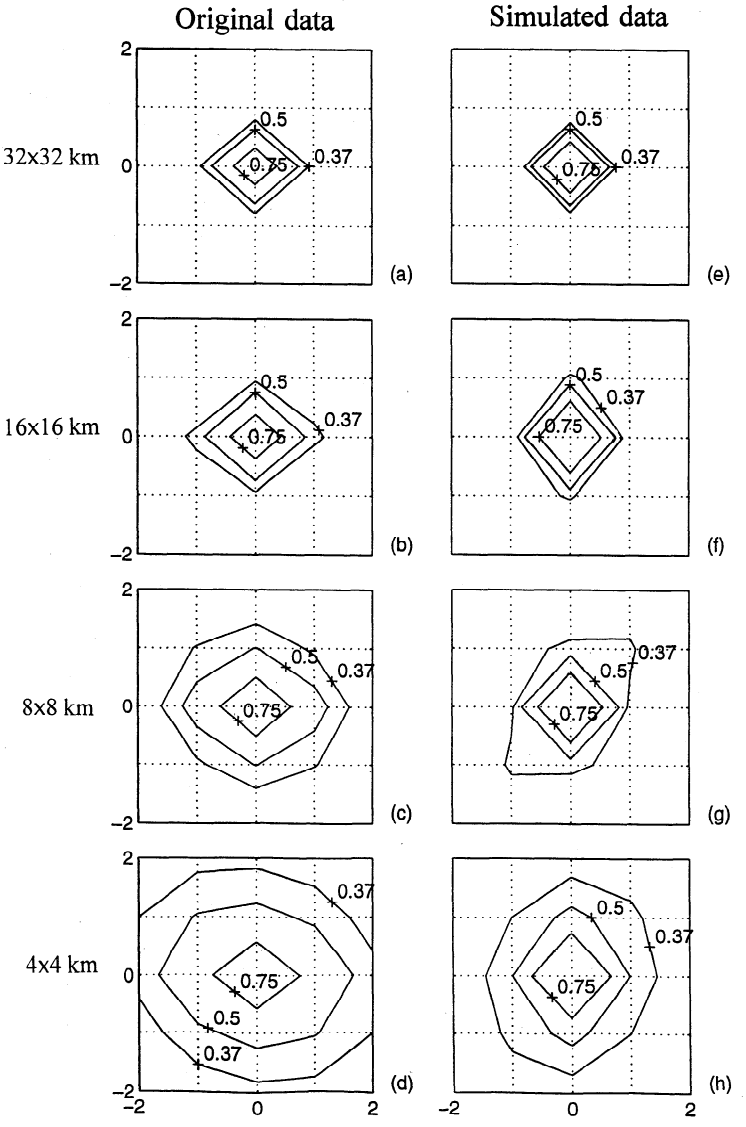

Figure 10. The 0300 UTC, June 27, 1985, data set. (a)–(d) Spatial correlation structure in the original rainfall field and its aggregates; (e)–(h) spatial correlation structure in the simulated fields, at scales 32×32 up to 4×4 km, respectively.

fields is better at larger scales. At the smallest analyzed scale, an exact match of points with nonzero rainfall intensities occurs in about 50% of the points, although from the visual-image comparison the overlapping area looks much larger. An example of the performance of the model in reconstructing intermittency for different thresholds is given in Figure 7. Here the fractional coverage of rain is plotted versus scale for simulations with different thresholds, together with the curve computed directly from the data set. Similar results are given in tabular form in Table 4. As mentioned in section 3.3, the threshold value of 0.25 mm/h was found to be optimal in the analysis of most data sets, so it was retained for all simulations.

5. Sensitivity Analysis

5.1. Objectives

A sensitivity analysis of the model was performed to test the effects of uncertainty in the estimated CAPE values, directional differences in the scaling parameterization, and the effects of possible further model simplifications. Specifically, the following tests were performed:

Sensitivity to CAPE. We examined the response of the aforementioned measures of the model performance to uncertainties in the CAPE values. CAPE values were varied in the range of approximately ± 20% of the measured (observed) values. For several selected

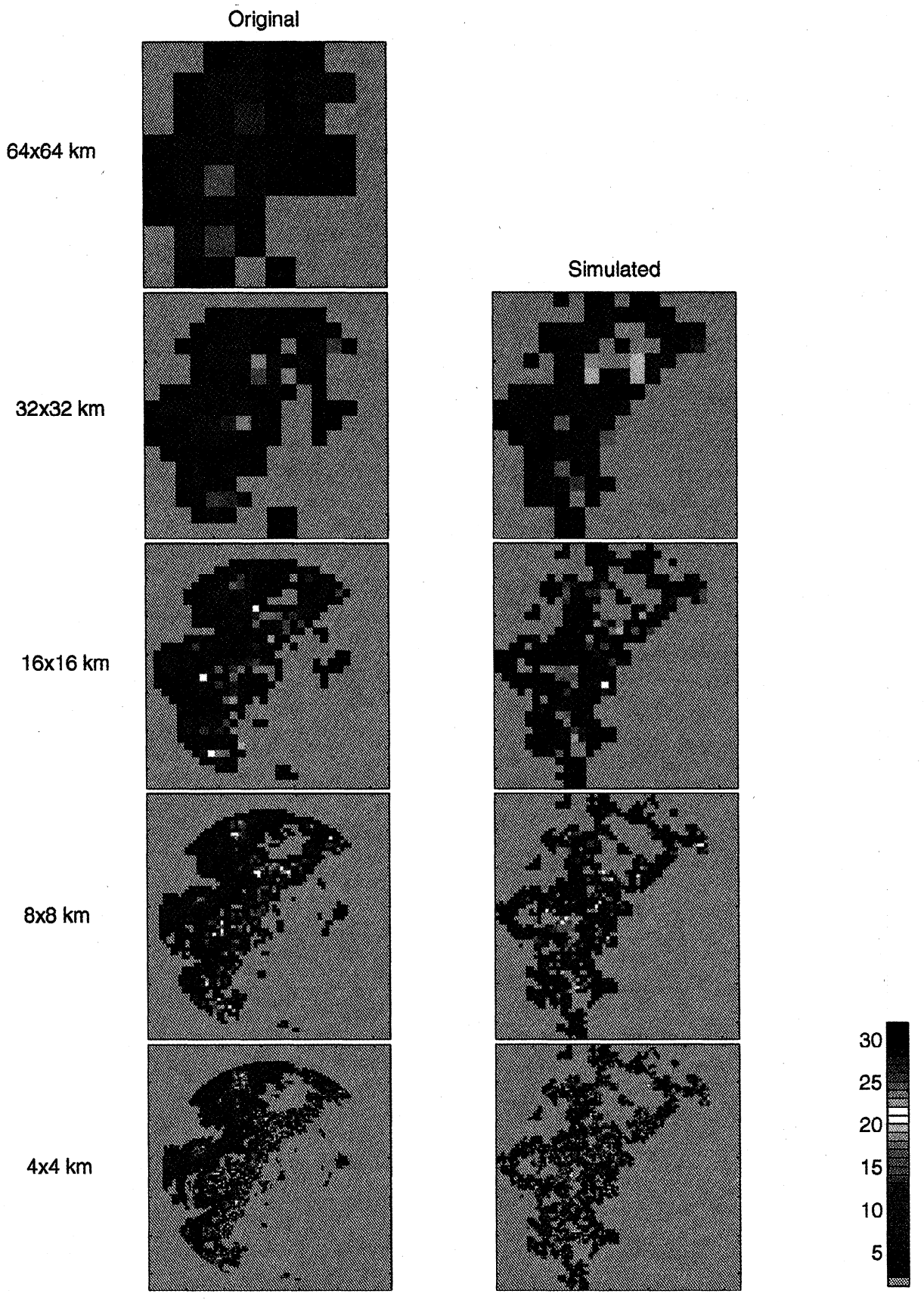

Plate 1. The 0300 UTC, June 27, 1985, data set. The left column shows images of the original rainfall field, and the right column shows images of the simulated rainfall fields over the range of scales analyzed.

Table 3. The "Figure of Merit" Measure Over Scales Calculated From One Simulation and From the Average of 100 Simulations

Scale	"Figure of Merit" Measure	
(km×km)	One Simulation	100 Simulations
32×32	0.73	0.74 (0.02)
16×16	0.65	0.66 (0.02)
8×8	0.55	0.57 (0.02)
4×4	0.48	0.49 (0.02)

The 0300 UTC, June 27, 1985, data set. For the 100 simulations the average moment values and their standard deviations (numbers in parentheses) are given.

CAPE values, the average value and standard deviation of each performance measure obtained from the 100 simulations were calculated and compared to those of the original rainfall field.

Sensitivity to directionality. Here we examined the effects of ignoring directional differences in the scaling parameterization. The model was initialized with (1) estimates of the directional parameters H_i and $\sigma_{1,i}$ $(i = 1, 2, 3)$ obtained from the original data set via a wavelet transform and (2) their average values $H = \sum_{i=1}^{3} H_i/3$, $\sigma_1 = \sum_{i=1}^{3} \sigma_{1,i}/3$. The simulated fields in each case were compared to the original rainfall fields.

Further reduction in parameterization. The possibility of further simplifying the model to just needing one parameter H (instead of H and σ_1), derived from the obtained relation with CAPE, was investigated. Parameter σ_m $(m \geq 1)$ is a scale-dependent parameter. In other words, the eventual relations found to exist between σ_m and CAPE are scale-dependent too. Our analysis has shown that in general the variability of standardized fluctuations described through the parameter σ_m increases as we go from finer to coarser scales. Parameter σ_1 (here at scale 8×8 km) was found to be linked to CAPE with a significant correlation coefficient (R=-0.73). However, as we go to coarser scales, σ_m estimates are less and less dependent on CAPE. Finally, at the 64×64 km scale, the standard deviation of standardized fluctuations σ_4 is almost independent of CAPE (R=-0.25), and is approximately constant. In other words, the variability of standardized fluctuations grows as we go to larger scales, and at the same time, it becomes less and less dependent on the storm intensity and type. This is illustrated in Figure 11. If the results of the model are not overly sensitive to the scale of variability of the standardized fluctuations that the model is initiated with, then we could assume that the only statistical parameter that has to be estimated from CAPE using equation (7) is the scale-invariant parameter H. Instead of estimating σ_1 from the obtained regression equation with CAPE, we can initialize our model with a constant σ_4 value, here σ_4=0.58 at scale of 64×64 km (see Figure 11) independently of storm type or intensity for the midwestern MCS considered in this study. This would be a desirable simplification in practical applications. The results of the sensitivity analysis for a case study are presented below.

5.2. Results From a Case Study

The 0300 UTC, June 27, 1985, data set, which was used to evaluate model performance in the previous section, was also used to report the results of the sensitivity analysis of the model. All results displayed in the tables that follow are results obtained from 100 runs of the model with the same set of initial parameters.

First, we tested model sensitivity to uncertainty in estimating the CAPE value. A representative CAPE value from the HET sounding site taken at 0300 UTC time was estimated to be 1584 m^2/s^2. Several CAPE values were then selected from the interval 1300–1900 m^2/s^2, as shown in Table 5. For each CAPE value, the statistical parameters H and σ_1 were estimated using regression equations (7) and (8). The model was then run 100 times for each selected CAPE value. Average values and standard deviations of the obtained model performance measures are given in Table 5. The table shows that in general the statistical measures of the

Table 4. Fractions of Rainy Areas For the Original and Reconstructed Rainfall Fields as a Function of the Threshold Value τ Used in the Simulation

Scale	Observed	Modeled Fraction With τ (mm/h)				
(km×km)	Fraction	0.10	0.25	0.50	0.75	1.00
64×64	0.61					
32×32	0.46	0.46 (0.01)	0.42 (0.01)	0.38 (0.01)	0.34 (0.01)	0.31 (0.01)
16×16	0.37	0.41 (0.01)	0.37 (0.01)	0.32 (0.01)	0.28 (0.01)	0.25 (0.01)
8×8	0.31	0.37 (0.01)	0.33 (0.01)	0.28 (0.01)	0.24 (0.01)	0.22 (0.01)
4×4	0.26	0.34 (0.01)	0.30 (0.01)	0.25 (0.01)	0.21 (0.01)	0.19 (0.01)

The 0300 UTC, June 27, 1985, data set. Values reported are average values from 100 simulation runs and numbers in parentheses indicate the standard deviations of the estimates.

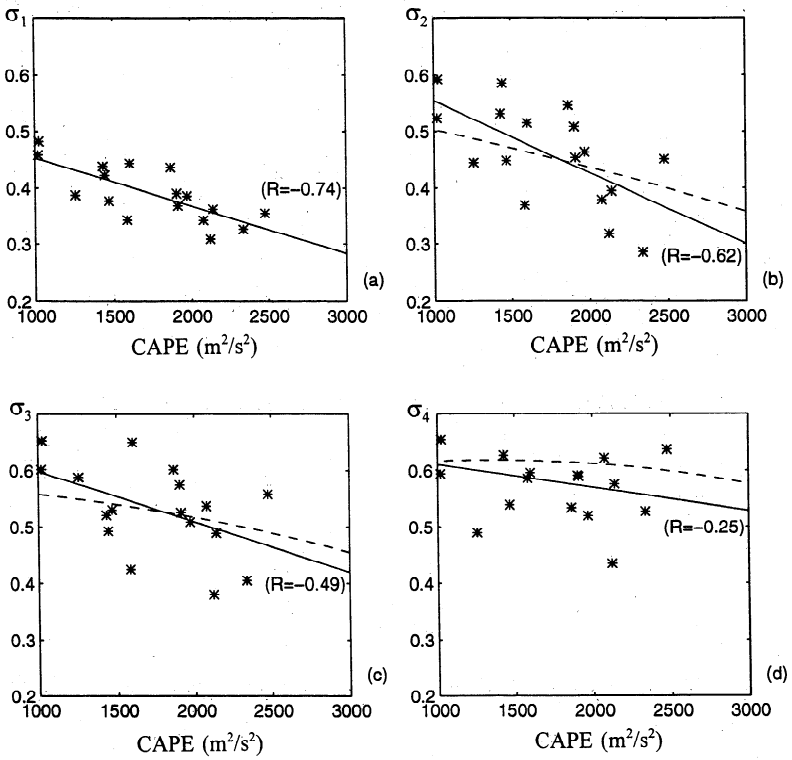

Figure 11. Scattergrams of σ_m versus CAPE at scales $m = 1, 2, 3, 4$. Dashed lines represent values calculated from $\sigma_m = 2^{(m-1)H}\sigma_1$, where H and σ_1 are estimated from equations (7) and (8) as functions of CAPE. Solid lines represent linear regression lines between σ_m and CAPE; associated correlation coefficients are also indicated in the figures.

Table 5. Model Sensitivity to Potential Errors (Due to Uncertainty) in CAPE Estimates

			Model Performance Measures					
CAPE (m^2/s^2)	H	σ_1	$\overline{\overline{X}}_0$ (mm/h)	$\sigma_{\overline{X},0}$ (mm/h)	$\overline{\overline{R}}_0$ (mm/h)	$\sigma_{\overline{R},0}$ (mm/h)	Fraction of Rainy Area	"Figure of Merit"
				For Measured Field				
			1.84	6.59	6.97	11.30	0.26	
				For Simulated Field				
1300	0.18	0.43	1.84	6.47 (0.35)	6.47 (0.22)	10.91 (0.79)	0.28 (0.01)	0.48 (0.02)
1400	0.19	0.42	1.84	6.44 (0.35)	6.41 (0.22)	10.83 (0.78)	0.28 (0.01)	0.48 (0.02)
1500	0.20	0.41	1.84	6.44 (0.35)	6.40 (0.21)	10.67 (0.78)	0.29 (0.01)	0.48 (0.02)
1584	0.20	0.40	1.84	6.39 (0.34)	6.21 (0.20)	10.54 (0.78)	0.30 (0.01)	0.49 (0.02)
1600	0.21	0.40	1.84	6.38 (0.34)	6.15 (0.20)	10.53 (0.77)	0.30 (0.01)	0.49 (0.02)
1700	0.22	0.39	1.84	6.36 (0.34)	6.12 (0.20)	10.48 (0.76)	0.30 (0.01)	0.49 (0.02)
1800	0.23	0.39	1.84	6.34 (0.34)	5.98 (0.20)	10.39 (0.75)	0.31 (0.01)	0.49 (0.02)
1900	0.24	0.38	1.84	6.28 (0.34)	5.94 (0.20)	10.29 (0.75)	0.31 (0.01)	0.50 (0.02)
				Maximum Relative Error (%)				
	20.00	7.50	0.00	1.72	4.40	3.56	3.40	2.03

The 0300 UTC, June 27, 1985, data set. Results are given for the 4×4 km scale where, in general, relative errors are the highest. CAPE=1584 m^2/s^2 is the value estimated from the HET sounding site. Values reported are averages over 100 simulations. The values in parentheses indicate the standard deviations of the estimates.

Table 6. Model Performance Measures Obtained From 100 Simulation Runs With All Six Parameters ($6P$) and With Two Parameters Only Representing Their Average Values ($2P$)

Model Performance Measure	Number of Parameters	Scale (km×km) 32×32	16×16	8×8	4×4
$\overline{\overline{X}}$, mm/h	($6P$)	1.84	1.84	1.84	1.84
	($2P$)	1.84	1.84	1.84	1.84
$\sigma_{\overline{X}}$, mm/h	($6P$)	3.78 (0.18)	4.52 (0.22)	5.24 (0.26)	5.96 (0.30)
	($2P$)	3.80 (0.19)	4.54 (0.22)	5.28 (0.26)	6.01 (0.29)
$\overline{\overline{R}}$, mm/h	($6P$)	4.30 (0.12)	4.85 (0.15)	5.33 (0.16)	5.71 (0.16)
	($2P$)	4.30 (0.11)	4.86 (0.14)	5.35 (0.15)	5.73 (0.16)
$\sigma_{\overline{R}}$, mm/h	($6P$)	4.79 (0.33)	6.27 (0.43)	7.83 (0.53)	9.41 (0.64)
	($2P$)	4.82 (0.35)	6.31 (0.43)	7.91 (0.53)	9.50 (0.63)
Fraction of rainy area	($6P$)	0.43 (0.01)	0.37 (0.01)	0.34 (0.01)	0.32 (0.01)
	($2P$)	0.43 (0.01)	0.38 (0.01)	0.34 (0.01)	0.32 (0.01)
"Figure of merit"	($6P$)	0.75 (0.02)	0.67 (0.02)	0.59 (0.02)	0.51 (0.02)
	($2P$)	0.74 (0.02)	0.66 (0.02)	0.58 (0.02)	0.51 (0.02)

The 0300 UTC, June 27, 1985, data set. Numbers in parentheses indicate the standard deviations of the estimates.

model performance are not very sensitive to small perturbations in CAPE values; a 20% range in CAPE gives rise to less than 10% error in the statistical measures of the simulated rainfall fields. As can be seen from the table, the results obtained for the fractional coverage and "figure of merit" measure are also very robust to variations in the CAPE values.

To test if model performance can be improved when directional differences in the scaling parameters are not ignored, the model was initialized with a set of "true" (instead of estimated from CAPE) scaling parameters. These parameters were obtained from the scaling analysis of the standardized rainfall fluctuations of the observed rainfall field: $H_1 = 0.247, H_2 = 0.258$, and $H_3 = 0.246; \sigma_{1,1} = 0.368, \sigma_{1,2} = 0.325$, and $\sigma_{1,3} = 0.283$. The results were compared to those obtained when the model was initialized with just two parameters representing their average values: $H = 0.250$ and $\sigma_1 = 0.325$. The results are presented in Table 6. The differences between these two simulations are insignificant, suggesting that the scaling parameterization of the model can be approximated with just two parameters at least for systems that have no significant linear structure. For systems with pronounced directionality

Table 7. Comparison of Results Obtained When the Model Was Initialized With Two Parameters ($2P$) or Just One Scaling Parameter ($1P$)

Model Performance Measure	Number of Parameters	Scale (km×km) 32×32	16×16	8×8	4×4
$\overline{\overline{X}}$, mm/h	($2P$)	1.84	1.84	1.84	1.84
	($1P$)	1.84	1.84	1.84	1.84
$\sigma_{\overline{X}}$, mm/h	($2P$)	3.81 (0.21)	4.62 (0.26)	5.48 (0.29)	6.39 (0.34)
	($1P$)	3.79 (0.20)	4.56 (0.24)	5.37 (0.29)	6.22 (0.34)
$\overline{\overline{R}}$, mm/h	($2P$)	4.36 (0.13)	5.01 (0.17)	5.63 (0.18)	6.21 (0.20)
	($1P$)	4.32 (0.12)	4.94 (0.15)	5.52 (0.17)	6.04 (0.19)
$\sigma_{\overline{R}}$, mm/h	($2P$)	4.85 (0.39)	6.51 (0.52)	8.41 (0.63)	10.50 (0.78)
	($1P$)	4.81 (0.37)	6.38 (0.48)	8.14 (0.60)	10.10 (0.75)
Fraction of rainy area	($2P$)	0.42 (0.01)	0.37 (0.01)	0.33 (0.01)	0.30 (0.01)
	($1P$)	0.43 (0.01)	0.37 (0.01)	0.33 (0.01)	0.30 (0.01)
"Figure of merit"	($2P$)	0.74 (0.02)	0.66 (0.02)	0.57 (0.02)	0.49 (0.02)
	($1P$)	0.74 (0.02)	0.66 (0.02)	0.58 (0.02)	0.50 (0.02)

The 0300 UTC, June 27, 1985, data set. Numbers in parentheses indicate the standard deviations of the estimates.

this approximation might not be appropriate and needs further assessment.

To investigate the effect of further possible model simplification (based on the assumption that the statistical variability of standardized rainfall fluctuations at the large scale is constant and independent of the storm intensity or type), 100 additional simulations were produced with parameters $\sigma_4 = 0.58$, and H defined from the regression equation with CAPE (equation (7)). With this assumption the scaling variability at any scale $m = 3, 2, 1$ can be derived from the following expression:

$$\sigma_m = \sigma_4 \times 2^{(m-4)H} = 0.58 \times 2^{(m-4)H} \qquad (9)$$

The obtained results are compared in Table 7 with the simulation results with both scaling parameters estimated from CAPE. Our conclusion is that there is no significant difference in model performance measures in these two cases, suggesting possible model simplification.

6. Conclusions

The simulation of spatial rainfall at scales in the range of 2×2 to 30×30 km is a major challenge to atmospheric modelers. Rainfall at these scales exhibits considerable spatial heterogeneity. This heterogeneity is of great interest for many hydrologic applications and is usually unresolved by physically based mesoscale meteorological models.

We have developed a model which has the ability to statistically reproduce rainfall variability at small scales. Our model is conditioned on large-scale rainfall averages and the physical characteristics of the rainfall event represented through the convective available potential energy (CAPE). This model is intended to be coupled with a mesoscale weather prediction model for the purpose of subgrid-scale parameterization of rainfall.

The ability of the model to reproduce small-scale rainfall variability was validated by comparing summary statistics and spatial pattern measures of simulated fields with those of the known rainfall fields observed during the PRE-STORM experiment. By the properties of the Haar wavelet transform, the first moment of rainfall is explicitly preserved at all scales. Other statistical measures and the spatial patterns themselves compared very well with the corresponding statistical properties and spatial patterns of the original fields. One of the most notable features of this model is its ability to reconstruct the fraction of the area covered with rain at all subgrid scales by means of one pretty robust threshold parameter.

All the results presented in this paper are based on a single event analysis and as such constitute only a limited performance evaluation of the proposed model. To fully assess the model performance, a study based on several storms and different storm types is planned in the future.

Acknowledgments. The authors gratefully acknowledge the help of Professor James A. Smith and his group at Princeton University in obtaining the PRE-STORM data used in this study. They also gratefully acknowledge the support of NSF (grant EAR-9117866), NOAA (grant NA46GP 0486), and NASA (grant NAG 5-2108 and a graduate Global Change Fellowship awarded to the first author). Supercomputer resources were kindly provided by the Minnesota SuperComputer Institute. The helpful comments of three anonymous reviewers were greatly appreciated.

References

Blanchard, D. O., Mesoscale convective patterns of the southern High Plains, *Bull. Am. Meteorol. Soc., 71*(7), 994-1005, 1990.

Cunning, J. B., The Oklahoma-Kansas Preliminary Regional Experiment for STORM-Central, *Bull. Am. Meteorol. Soc., 67*(12), 1478-1486, 1986.

Johnson, K. D., D. Entekhabi, and P. S. Eagleson, The implementation and validation of improved landsurface hydrology in an atmospheric general circulation model, *Rep. 344*, Ralph M. Parsons Lab., Mass. Inst. of Technol., Cambridge, 1991.

Klug, W., G. Graziani, G. Grippa, D. Pierce, and C. Tassone, Evaluation of long term atmospheric transport models using environmental radioactivity data from the Chernobyl accident, *The ATMES Report*, Elsevier, New York, 1992.

Kumar P., and E. Foufoula-Georgiou, A multicomponent decomposition of spatial rainfall fields, 1. Segregation of large- and small-scale features using wavelet transforms, *Water Resour. Res., 29*(8), 2515-2532, 1993a.

Kumar P., and E. Foufoula-Georgiou, A multicomponent decomposition of spatial rainfall fields, 2. Self-similarity in fluctuations, *Water Resour. Res., 29*(8), 2533-2544, 1993b.

Kumar, P., and E. Foufoula-Georgiou, Characterizing multiscale variability of zero intermittency in spatial rainfall, *J. Appl. Meteorol., 33*(12), 1516-1526, 1994.

Mallat, S. G., A theory for multiresolution signal decomposition: The wavelet representation, *IEEE Trans. Pattern Anal. Mach. Intel., 11*(7), 674-693, 1989.

Perica, S., and E. Foufoula-Georgiou, Linkage of scaling and thermodynamic parameters of rainfall: Results from midlatitude mesoscale convective systems, *J. Geophys. Res., 101*, 7431-7448, 1996.

Thomas, G., and A. Henderson-Sellers, An evaluation of proposed representations of subgrid hydrologic processes in climate models, *J. Clim., 4*, 898-910, 1991.

E. Foufoula-Georgiou, St. Anthony Falls Laboratory, Department of Civil Engineering, University of Minnesota, Mississippi River at 3rd Ave. SE, Minneapolis, MN 55414

S. Perica, NOAA/NWS/Hydrologic Research Laboratory, 1325 East-West Highway, Silver Spring, MD 20910

(Received November 1, 1995; revised May 5, 1996; accepted May 30, 1996.)